

# Corrosion behaviour of carbon steel in the Tournemire clay

F. Foct<sup>a</sup>, J. Cabrera<sup>b</sup>, W. Dridi<sup>a</sup>, S. Savoye<sup>b</sup>

<sup>a</sup> EDF R&D MMC, Site des Renardières, 77818 Moret sur Loing Cedex, France  
tel : 33 (0)1 60 63 69 65 ; fax : 33 (0)1 60 73 68 89 ; e-mail : francois.foct@edf.fr

<sup>b</sup> IRSN/DEI/SARG bat 76/2 BP 17 92262 Fontenay-aux Roses, France  
tel : 33-(0)-1-58-35-90-10 ; fax : 33-(0)-1-58-35-71-35 ; e-mail : sebastien.savoye@irsn.fr

## **Abstract**

Carbon steels are possible materials for the fabrication of nuclear waste containers for long term geological disposal in argillaceous environments. Experimental studies of the corrosion behaviour of such materials has been conducted in various conditions. Concerning the numerous laboratory experiments, these conditions (water and clay mixture or compacted clay) mainly concern the bentonite clay that would be used for the engineered barrier. On the opposite, only few in-situ experiments has been conducted directly in the local clay of the repository site (such as Boom clay...). In order to better estimate the corrosion behaviour of carbon steels in natural clay site conditions, an experimental study has been conducted jointly by EDF and IRSN in the argillaceous French site of Tournemire. In this study, A42 carbon steel specimens have been exposed in 3 different zones of the Tournemire clay formation. The first type of environmental conditions concerns a zone where the clay has not been affected by the excavation (EDZ) of the main tunnel neither by the main fracture zone of the clay formation. The second and third ones are located in the EDZ of the tunnel. In the second zone, an additional aerated water flows from the tunnel, whereas it does not in the third place. Some carbon steel specimens have been extracted after several years of exposure to these conditions. The average corrosion rate has been measured by the weight loss technique and the pitting corrosion depth has been evaluated under an optical microscope. Corrosion products have also been characterised by scanning electron microscopy and X-ray diffraction technique. Results are then discussed regarding the surrounding environmental conditions. Calculations of the oxygen transport from the tunnel through the clay and of the clay resaturation can explain, in a first approach, the corrosion behaviour of the carbon steel in the different tested zones.

**Keywords :** Nuclear waste storage, carbon steel, clay, general corrosion, pitting corrosion.

## **Introduction**

The argillaceous rocks are considered as potential geological formations for the nuclear waste disposal, due to their good confinement properties. Prior to final disposal, the wastes will be packed in metallic containers which will have to isolate the wastes from the geological environment during 1000 years to 10 000 years depending on the concepts. In France, the reference materials for the containers are the carbon and low alloy steels. In this context, Electricité de France R&D has undertaken a research project on such nuclear waste disposal concepts. One task of this project is conducted jointly with the IRSN (laboratories of the French nuclear regulation agency). It concerns the evaluation of the corrosion behaviour of A42 carbon steels in the clay of the site of Tournemire [1] (argillaceous site located in the south of France). It is an important issue since in-situ corrosion experiments (such as Mol laboratory [2]) are seldom. This paper presents the results obtained after 2 years of exposure of the steel specimens to the clay.

## Experimental procedure

### *Studied Material*

The material chosen for this study is a A42 carbon steel. It is a potential material for the over packing of the high activity, long life nuclear waste container in the main concept proposed by the French agency for nuclear waste disposal (ANDRA). The chemical composition and the mechanical characteristics of this steel are presented in Table 1.

Table 1 : Chemical composition (wt. %) and mechanical characteristics of the A 42 carbon steel.

	C	Mn	P	S	Si	Ni	Cr	Mo	R <sub>p0.2</sub> (MPa)	R <sub>m</sub> (MPa)	A%
NF A 35-501	≤ 0.2	≤ 1.6	≤ 0.045	≤ 0.045	≤ 0.45	-	-	-	≥ 255	400 - 540	≥ 22
analysis	0.178	0.59	0.013	0.033	0.14	0.04	0.04	<0.01	-	-	-

The microstructure of the A42 steel has been observed in the transversal direction of the plate after metallurgical etching. The A42 steel presents a mixed ferrite and perlite microstructure (Figure 1). The average grain size is close to 20  $\mu\text{m}$  and the microstructure does not exhibit a specific texture.

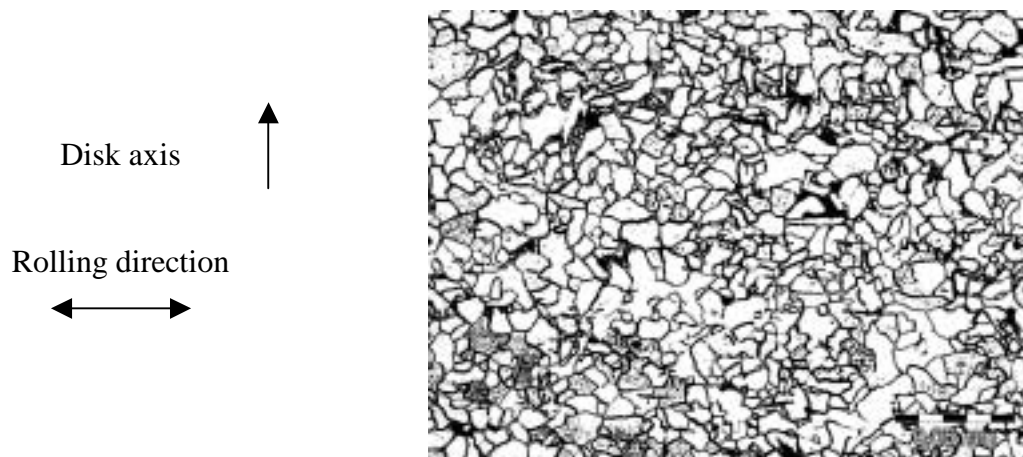


Figure 1 : microstructure of the A42 steel used in this study.

### *Specimens*

The specimens used for the corrosion tests are 42 mm diameter disks with a 3 mm thickness. They have been polished with a 600 grind paper.

### *Environmental conditions*

#### *Situation and characteristics of the Tournemire site and of the different drillings*

The argillaceous site of Tournemire (Aveyron, France) is constituted of a 250 m thick argillaceous formation surrounded by calcareous aquifers. A 2 km long, 100 years old railway tunnel ensures the access to this formation. The geological characteristics of this site are detailed in [1].

The corrosion tests consist in placing the carbon steel samples in different drillings excavated in the clay from the tunnel. The specimens were placed at the end of the drillings. They are spaced from each other by clay cylinders and powder. The drillings were then filled with the site clay. Eight 46 mm diameter drillings were excavated in two different zones (Figure 2).

The first zone (horizontal drillings named CR4, CR5 and CR6) is located 10 m far from the tunnel. It is away from the excavation damaged zone (EDZ) and is therefore representative of a natural argillaceous site. The second and third zones (vertical drillings named CR1, CR2, CR3, CR7 et CR8) are situated under the tunnel, in a highly fractured clay with a water flow (third zone only).

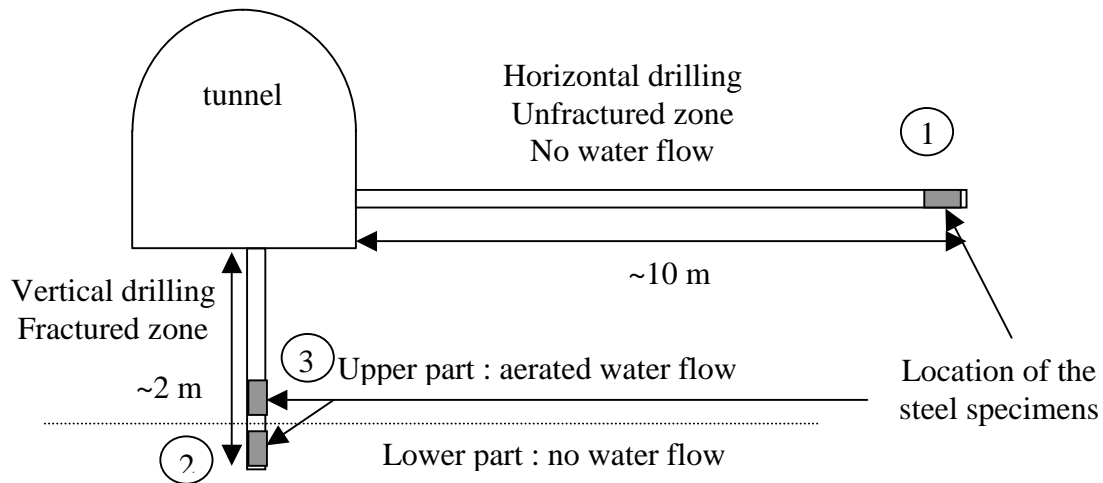


Figure 2 : Schematic representation of the drillings and testing zones in the tunnel of Tournemire.

#### *Disposition of the specimens in the different drillings*

Five carbon steel specimens were placed in each drilling. The distance between two specimens is about 5 cm. In the horizontal drilling CR4, the 5 specimens were placed at the end of the drilling. In the vertical drilling CR3, 2 specimens were placed at the end of the drilling, below the fractured zone where not convective flow of water occurs, and 3 specimens were placed 50 cm higher, in the EDZ, where the convective flow of water takes place.

#### *Clay composition*

The Tournemire clay has an average water content of 3 wt.% and a density of 2.6. It is mainly composed of argillaceous phase (40 – 60% mainly illite and smectite), quartz (15 – 20 %), carbonate (10 – 15% as calcite), pyrite (0 –3 %) and organic material (1%). The chemical composition of the Tournemire clay is presented in Table 2 [1].

Table 2 : Chemical composition (oxide %) of the Tournemire clay [1].

	SiO <sub>2</sub>	Al <sub>2</sub> O <sub>3</sub>	MnO	MgO	CaO	Na <sub>2</sub> O	K <sub>2</sub> O	TiO <sub>2</sub>	Fe <sub>2</sub> O <sub>3</sub>
Unfractured clay	50.5	17.6	0.05	2.0	7.3	0.4	3.1	1.0	5.7
Fractured clay	49.0	15.8	0.04	1.7	9.7	0.3	2.9	0.9	5.8

#### *Chemical composition of the water flowing through the drilling CR3*

Some water flowing through the drilling CR3, located in the EDZ, was taken to proceed to its chemical analysis. It is a weakly alkaline and mineralised water with low chloride content of 3,9 ppm (Table 3) [1].

Table 3 : Chemical composition (mmol/l) of the water flowing through the EDZ below the tunnel of Tournemire (drilling CR3) [1].

pH	[K] <sub>T</sub>	[Mg] <sub>T</sub>	[Ca] <sub>T</sub>	[Na] <sub>T</sub>	[Sr] <sub>T</sub>	[Si] <sub>T</sub>	[F]	[Cl]	[NO <sub>3</sub> <sup>-</sup> ]	[SO <sub>4</sub> <sup>-2</sup> ]
7.8	0.12	0.74	1.26	0.51	0.004	0.11	<0.005	0.11	0.01	0.57

T : indicates the total concentration of the element.

#### *Specimens extraction procedure*

The specimens were extracted after two 2 years. 20 cm diameter over drillings have been realised at the initial drillings (46 mm) places in order to extract the specimens. Once extracted, the specimens and the surrounding clay have been packed under nitrogen cover in sealed aluminium bags.

#### *Measurements and examinations*

The following measurements and examinations have been conducted on the specimens :

- Determination of the average corrosion rate by weight loss measurement after washing in water and chemical dissolution of the oxides in a 50 % hydrochloric acid solution added with 5 g/l hexamethylenetetramine.
- Determination of the type of corrosion under an optical microscope.
- Determination of the maximum pit depth after chemical dissolution of the oxides under an optical microscope by measuring the sample displacement when focussing on the bottom of the pit and near to the pit.
- Identification of the different types of oxides by X ray diffraction analysis.
- Observation of the oxide morphology under a scanning electron microscope (SEM) on transversal cuts of the samples.
- WDS analysis on transversal cuts of the samples to realise elements cartography.

## **Results**

#### *General corrosion*

The aspect of the specimens after extraction from the clay is presented in Figure 3 for each condition. The yellow – brown colour of the clay reveals the presence of corrosion products. The clay stickiness to the steel is variable, very adherent in some place and easily removed in others. In the fractured zone where the water flows, the clay is more adherent and humid.



Figure 3 : aspect of the samples after extraction from the clay.

After ultrasonic cleaning in water, the specimens present a surface entirely covered by a dark brown compact oxide.

The average corrosion rate has been measured by the weight loss technique (Table 4). The average corrosion rate measured in the unfractured zone is fairly constant (13 to 17  $\mu\text{m}/\text{year}$ ) and is coherent with the expected rate for aerated conditions [3]. The results are much more variable in the EDZ (vertical drilling CR3). The corrosion rate was found relatively low in the lower part of the drilling, where no water flows. In the higher part of the drilling where the water flows, the corrosion rate is much higher (39  $\mu\text{m}/\text{year}$ ).

Those variations in corrosion rate are probably due to the different environmental conditions between the three tested zones (fractures, water flow).

Table 4 : Estimation of the average corrosion rate of the carbon steel with the weight loss technique.

drilling	zone	weight loss ( $\text{g}/\text{cm}^2$ )	$\Delta e$ ( $\mu\text{m}$ )	rate ( $\mu\text{m}/\text{an}$ )	max pit depth D ( $\mu\text{m}$ )	$P = D/\Delta e$
CR3	EDZ + water flow	0.06192	78.8	39.4	196	2.5
	EDZ	0.00811	10.3	5.2	72	7
CR4	Unfractured clay	0.02053	26.1	13.1	164	6.3
		0.02701	34.4	17.2	150	4.4

#### *Pitting corrosion*

The maximum pit depth D has been measured on every sample (Table 4). The pitting factor P is then defined for each specimen as the ratio between the maximum pit depth and the average corrosion depth. The maximum pit depth is similar for the two specimens placed in the unfractured zone (150 to 164  $\mu\text{m}$ ). It is higher in the EDZ where there is a water flow and lower in the bottom part of the vertical drilling.

The pits observed on the A42 steel exposed to the Tournemire clay have a hemispherical shape (Figure 4) whatever the tested zone (fractured or not).

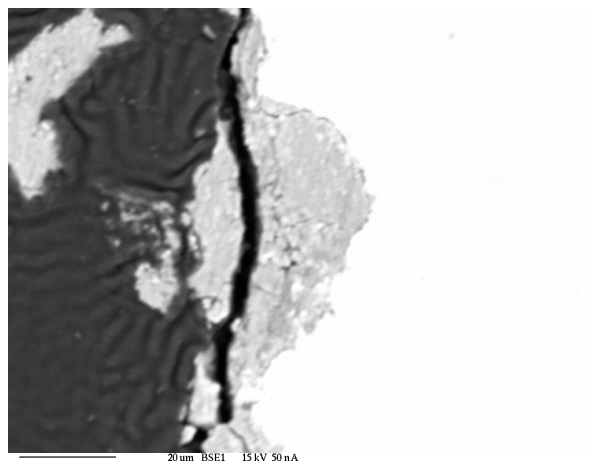


Figure 4 : SEM observation in back scattered electrons of a pit on a transversal cut of a specimen.

#### *Oxide layer composition*

The composition of the oxide layer has been determined by X-Ray diffraction after removing the adherent clay. Goethite ( $\text{FeO}(\text{OH})$ ) is always observed with sometimes iron hydroxide ( $\text{Fe}(\text{OH})_3$ ) and some minerals from the clay. The important quantity of  $\text{Fe}^{3+}$  in the oxide layer proves that the corrosion took place in aerated conditions during the two years of exposition.



*Cartography of the different elements in the clay and oxide layer*

The WDS cartography of the different elements (Figure 5) show that iron is present in every observed part of the specimens : metal, oxide and clay. Nevertheless, the higher the distance from the iron matrix is, the lower the iron content is. Since iron oxide, as  $Fe_2O_3$ , is a compound of the Tournemire clay (Table 2), it cannot be distinguish between the part of the iron observed in the clay coming from the corrosion of the steel and that naturally present in the clay. The oxygen cartography shows an enriched area near the steel corresponding to the oxide, and a less oxygen concentrated region which corresponds to the clay. The presence of Si and Al enables to identify the clay which they are the main constitutive elements with oxygen.

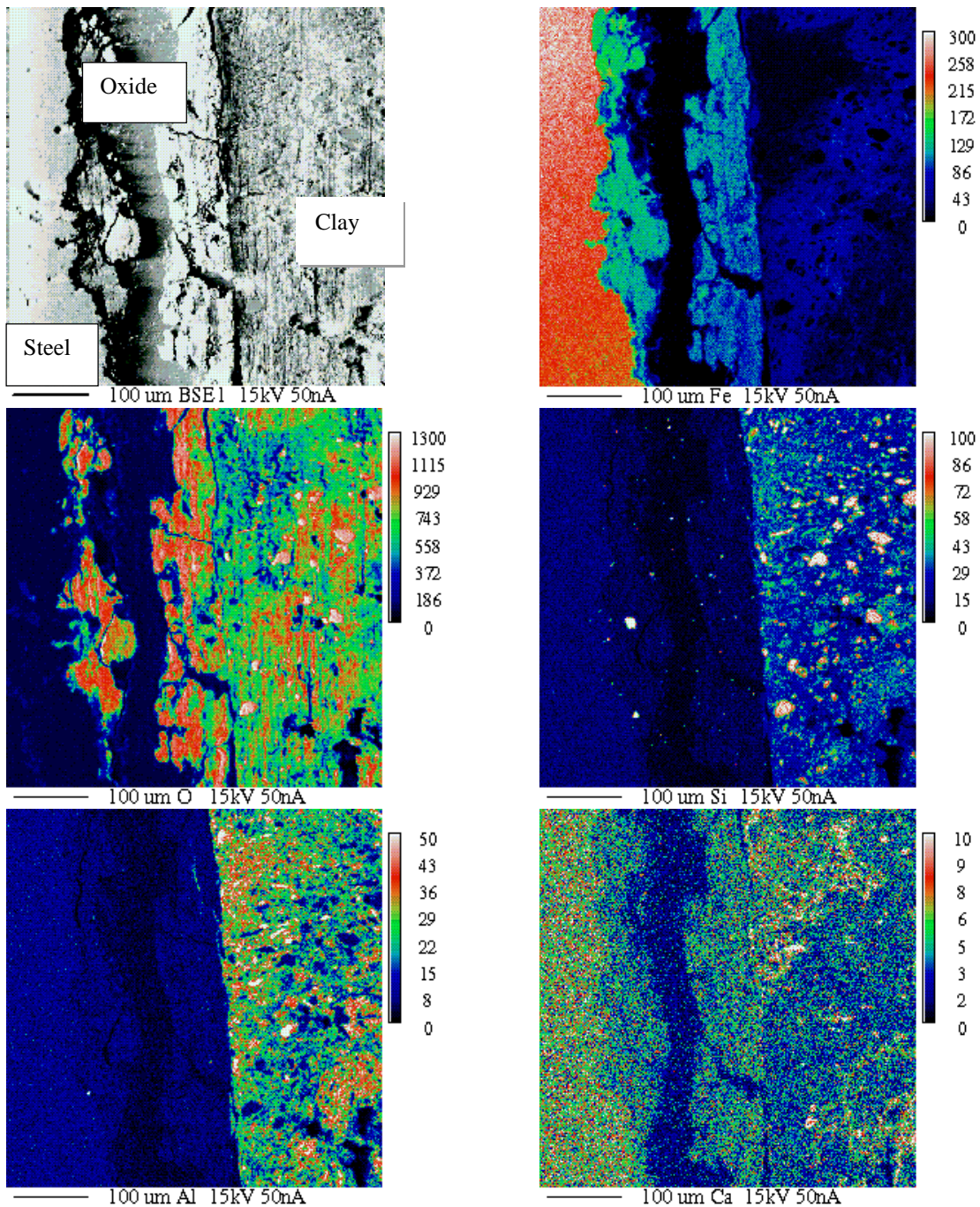


Figure 5 : WDS cartography of Fe, O, Si, Al, Ca in the oxide and clay surrounding a specimen.

On the unfractured clay, two parts can be distinguished in the oxide layer which total thickness is close to 80  $\mu\text{m}$ . The first one ( $\sim 40$   $\mu\text{m}$  thick) is located at the interface with steel and does not contain any Si or Al (clay free oxide). The second (also 40  $\mu\text{m}$  thick) is located at the interface with clay, and presents an important Si and Al content (mixed iron oxide and clay zone). The interface between these two types of oxides may correspond to the original interface between steel and clay. The inner layer of the oxide would then correspond to the fraction of oxide which has grown in place of the corroding steel and the outer oxide layer to the fraction of oxide which has grown inside the clay due to the metal / oxide volume expansion.

Such an oxide structure has been observed in the three different conditions, but the thickness of the different layers could not be measured for the specimens exposed to the fractured zone because of disbonding between oxide, metal and clay during the preparation of the specimens.

## Discussion

### *General corrosion of the carbon steel*

The high corrosion rate and the nature of the oxides grown on the specimens indicate that the environmental conditions in the drillings were aerated during the main part of these two first years of experiment. These aerated conditions are partly due to the air occluded in the clay porosity (micro and macro) during the filling of the drillings. The available quantity of oxygen around the steel specimens depends on the filling clay density and is roughly the same for the 3 tested zones. The oxygen occluded in the drillings is consumed by the corrosion of the carbon steel, leading to anoxic conditions. If the oxygen available for the corrosion only comes from the air occluded in the filling clay, the corrosion rates should be more or less the same in the three tested zones. The corrosion rates measured in the different drillings vary of one order of magnitude depending on the tested zone. Therefore, there are additional transport phenomena that bring different quantity of oxygen to the tested zones. Three scenarios are proposed hereafter to estimate the oxygen transport conditions in the drillings and their consequences on the steel corrosion rate.

### Unfractured zone (zone 1)

The general corrosion rate measured on the carbon steel located in the unfractured clay ( $\sim 15$   $\mu\text{m}/\text{year}$ ) is coherent with the semi empirical model proposed by GRAS [4, 5] for the oxic conditions (Figure 6). One can therefore imagine that the conditions inside the horizontal drilling stayed aerated during the two first years of the test. The presence of macroscopic cavities in the filling clay of this drilling is coherent with this scenario and indicates that a significant quantity of oxygen was available for corrosion. Moreover, the important porosity of the filling clay may allow a significant diffusion of oxygen along the drilling from the tunnel to the steel specimens during the resaturation of the filling clay. Some macroscopic cavities have been observed in the filling clay and they were not filled with water after two years. This observation confirms that the resaturation of the clay was not completed after two years. The occurrence of a gas phase transport mechanism for oxygen income to the steel specimens is therefore highly probable.

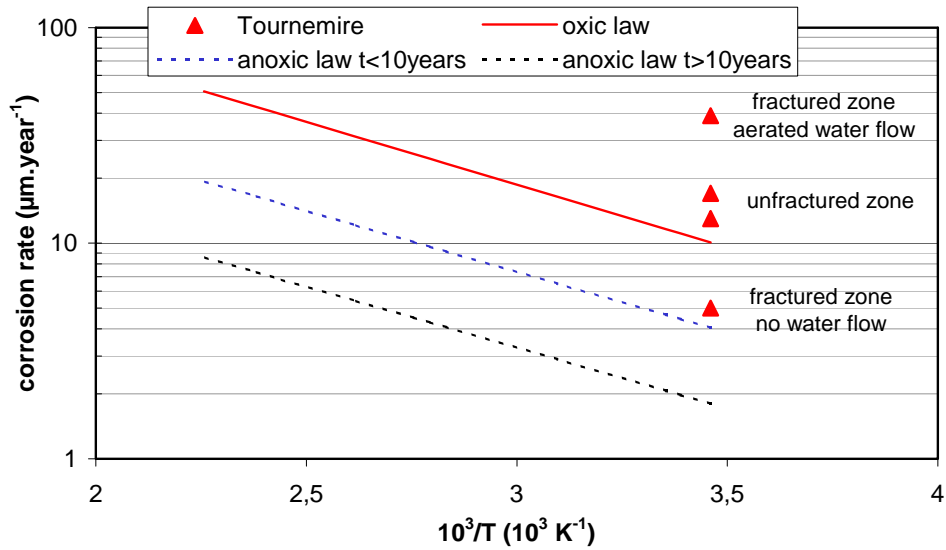


Figure 6 : Comparison between the corrosion rates measured at Tournemire and those expected with the empirical corrosion model [4].

In order to verify this assumption, the quantity of oxygen which can diffuse along the 10 m horizontal drilling up to the steel specimens has been calculated. The calculation has been made with a code developed for transport in unsaturated porous media [6]. The following hypothesis has been taken for the filling clay, considering that its compaction is poor :

- Intrinsic filling clay permeability<sup>1</sup> :  $10^{-15} \text{ m}^2$  ;
- liquid phase oxygen diffusion coefficient :  $D_{O_2} = 10^{-10} \text{ m}^2\text{s}^{-1}$  ;
- clay porosity : 35 % ;

The limit conditions are the following :

- the filling clay is in equilibrium with the tunnel atmosphere (3 tested relative humidity (RH) : 75 % ; 80 % and 85 %) ;
- $P_{O_2}$  drilling entry :  $2 \cdot 10^4 \text{ Pa}$  ;
- $P_{O_2}$  initial in the drilling :  $2 \cdot 10^4 \text{ Pa}$  ;
- $P_{O_2}$  drilling end : 0 (all the arriving oxygen is immediately used for the corrosion).

The evolution of the oxygen flux near the specimens is presented in Figure 7 for different relative humidity. The quantity of oxygen available for the steel corrosion is equal to the integral of the flux during two years : 0.004 mol for 85% RH, 0.009 mol for 80% RH or 0.012 mol for 75% RH. These quantity of oxygen correspond to a general corrosion depth varying between 2.5  $\mu\text{m}$  and 8  $\mu\text{m}$  for five 30  $\text{cm}^2$  specimens placed at the end of the drilling. The results of the calculation are consistent with the measured corrosion depth after two years (30  $\mu\text{m}$ ), considering that the calculation does not take into account the occluded oxygen in the filling clay nor the macroscopic voids in the drilling which can accelerate the oxygen transport. Hence this calculation validates the scenario where the filling clay is not resaturated after 2 years, allowing an important oxygen ingress to the specimens which keeps aerated conditions during this period.

<sup>1</sup> : After compaction, the filling clay presents some cavities, therefore we consider it behaves like an EDZ. We then chose permeability  $K_1$  of  $10^{-8} \text{ m/s}$ , average value measured in the EDZ of Tournemire [1]. The deduced intrinsic permeability of the clay is  $10^{-15} \text{ m}^2$ .



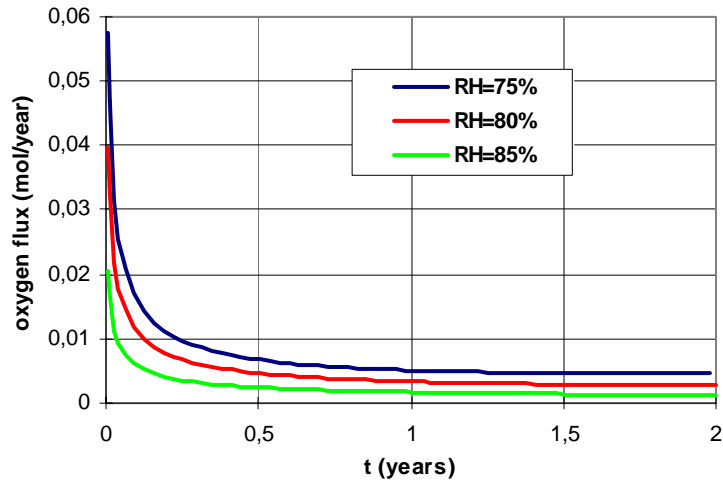


Figure 7 : Evolution of the oxygen flux at the end of the 10 m long horizontal drilling.

#### Fractured zone, lower part (zone 2)

The corrosion rate (5  $\mu\text{m}/\text{year}$ ) is slower in the lower part of the vertical drilling (in the fractured zone, below the water flow) than in the unfractured zone. In this testing zone, the clay seems almost saturated with water and no void can be seen. The resaturation of the drilling may have been accelerated by the water flow in the upper part of the drilling. In these conditions, the gas phase transport of oxygen from the tunnel through the filling clay should have been very limited. Therefore, the oxygen available for the steel corrosion probably comes from the air occluded in the clay and from the liquid phase diffusion from the tunnel through the filling clay.

The quantity of oxygen diffusing to the specimens through the lower 50 cm of the vertical drilling (below the flowing water zone) has been calculated in order to test this scenario. The same hypothesis as those of the previous simulation were taken into account for this calculation. The limit conditions are the following :

- Water saturated clay ;
- $P_{\text{O}_2}$  entry bottom fractured zone :  $10^4$  Pa (oxygen content of the flowing water (estimated at 4 ppm)) ;
- $P_{\text{O}_2}$  in the clay at  $t=0$  : 0 (the calculation only takes into account the oxygen arriving to the specimens from the tunnel, and not the air occluded in the filling clay) ;
- $P_{\text{O}_2}$  near the specimens : 0 (all arriving  $\text{O}_2$  is immediately used for the corrosion).

In these conditions, the oxygen flux near the specimens is constant :  $2.9 \cdot 10^{-17}$  mol/year. Hence, the quantity of oxygen arriving to the steel by liquid diffusion during two years can be neglected. This calculation shows that, once the occluded oxygen is consumed by the corrosion, the oxygen ingress from the tunnel is almost zero : anoxic conditions are then reached. The proposed scenario is therefore consistent with the experimental observations in this place where an average corrosion rate of 5  $\mu\text{m}/\text{year}$  was measured.

#### Fractured zone, upper part (zone 3)

The corrosion rate measured in the upper part of the fractured zone (flowing water zone) is higher than that expected by the empirical model (Figure 6). This behaviour can be explained by the aerated water convective flow coming from the surface of the tunnel and going through this fractured zone. This keeps aerated conditions which can accelerate the carbon steel corrosion. The quantity of oxygen coming through the clay to the steel specimens has been

calculated in these conditions in order to verify this scenario. The same hypothesis for the filling clay as those of the previous simulation were taken into account for this calculation. The limit conditions are the following :

- Water saturated clay ;
- $P_{O_2}$  drilling entry :  $2 \cdot 10^4$  Pa (equilibrium with the tunnel atmosphere) ;
- $P_{O_2}$  in the drilling :  $10^4$  Pa (oxygen content of the flowing water (estimated at 4 ppm) ; the calculation does not take into account the air occluded in the filling clay) ;
- Aerated water flux : 25 ml/h.

The oxygen flux near the specimens is constant : 0.0275 mol/year and comes almost only from the water flow. In two years, 0.055 mol of oxygen come to the three 30 cm<sup>2</sup> specimens. It corresponds to an average corrosion depth of 60 μm, assuming the whole oxygen is consumed by the corrosion of the 3 specimens. This value is very close to that measured on one of these specimens (80 μm). Hence, the main reason for the high carbon steel corrosion rate in this part of the vertical drilling, is the oxygen flux caused by the convective aerated water flow.

#### *Pitting corrosion of the carbon steel*

The maximum pit depth measured on each extracted specimen varies from 70 μm to 200 μm depending on the tested zone. The evolution of the deduced pitting factor (P = ratio between the maximum pit depth and the general corrosion depth) versus the general corrosion depth is presented in Figure 8. The results are consistent with the semi empirical model [3, 4] and are one order of magnitude below the envelope curve proposed for the estimation of the maximum pit depth.

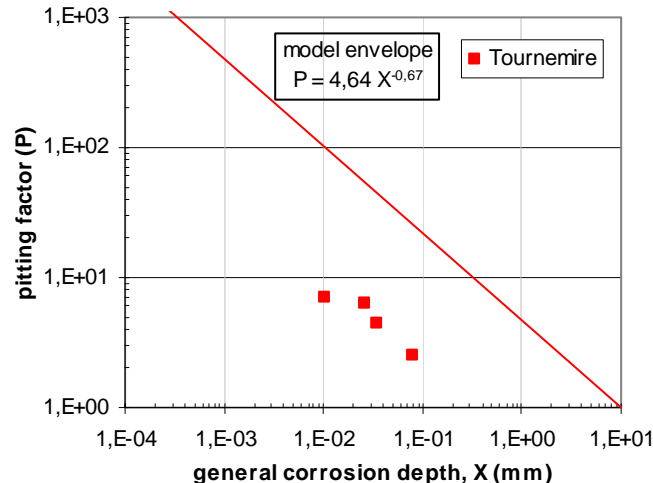


Figure 8 : Evolution of the pitting factor of carbon steels vs. the general corrosion depth.

### **Conclusion**

This paper presents the results obtained after 2 years of exposition of carbon steel specimens in the clay of Tournemire. The general corrosion rate of the steel tightly depends on the oxygen transport phenomena through the filling clay where the specimens are placed.

- If the clay is not resaturated with water (zone 1), the gas phase oxygen transport can be sufficient to maintain aerated conditions leading to a 15 μm/year corrosion rate consistent with the field experience in aerated clay.

- Once the filling clay saturated with water (zone 2), the oxygen ingress by liquid diffusion through the clay can be neglected and anoxic conditions are reached. The measured corrosion rate (5  $\mu\text{m}/\text{year}$ ) is due to an aerated phase (until the occluded oxygen is consumed) and an anoxic phase (once the occluded oxygen is consumed).
- In saturated clay, the occurrence of a convective flux of aerated water (zone 3) can bring enough oxygen to maintain oxic conditions and lead to higher corrosion rate (40  $\mu\text{m}/\text{year}$ ) than that expected from the literature in static conditions.

In these conditions, some corrosion pits are observed on the carbon steel with a maximum depth reaching 200  $\mu\text{m}$  after 2 years. The evolution of the deduced pitting factor is coherent with the empirical model [3] : it decreases as far as the general corrosion increases.

### References

- 
1. J. Cabrera Nunez, C. Beaucaire, G. Bruno, L. De Windt, A. Genty, N. Ramambasoa, A. Rejeb, S. Savoye, P. Volant, " PROJET TOURNEMIRE - Synthèse des programmes de recherche 1995 - 1999 ", IRSN report DPRE/SERGD 01 – 19.
  2. B. Kursten, P. Van Iseghem, Corrosion 99 Congress, Communication n°473, San Antonio, 25-30 april 1999.
  3. F. Foct, J.-M. Gras, International Workshop "Prediction of long term corrosion behaviour in nuclear waste systems", Cadarache, France, 26-29 November 2001, *EFC Series 36* (2002).
  4. J. M. Gras, « Modélisation semi-empirique de la corrosion des aciers non alliés en situation de stockage. Actualisation du modèle EDF 1996 », EDF report n° HT-40/01/004/A (2001).
  5. J.-M. Gras, C. R. Physique 3, 891-902 (2002).
  6. W. Dridi, « Couplage entre corrosion et transport diphasique dans un milieu poreux : application à l'évolution d'un stockage des déchets radioactifs », PhD thesis of ENPC, to be published (2004).